Oxidation of Isoprene to Methyl vinyl ketone and Methacrolein via Hydroxyl Radical: A Regenerative Mechanism for the Hydroxyl Radical

by

Richard Howell

November, 2013

Director of Thesis/Dissertation: (Libero Bartolotti)

Major Department: (Chemistry)

Isoprene is an important molecule in atmospheric chemistry. Belonging to a class of molecules known as volatile organic compounds, it undergoes reactions with several different oxidizers in the atmosphere, including OH(hydroxyl radical). In 2005 the concentrations of isoprene, OH and a few other isoprene derivatives were measured above the Amazonian rain forest. OH was found to be in concentrations far above levels predicted by computer models. As a result, a mechanism involving a 1,5-H shift was proposed to help explain the high levels of OH. Four reaction pathways, two different conformations of two different oxidation products, for the oxidation of isoprene and regeneration of the hydroxyl radical involving a 1,5-H shift mechanism were studied using the M062X density functional and the maug-cc-PVTZ basis set.

Oxidation of Isoprene to Methyl vinyl ketone and Methacrolein via Hydroxyl Radical: A Regenerative Mechanism for the Hydroxyl Radical

A Thesis

Presented To the Faculty of the Department of Chemistry

East Carolina University

In Partial Fulfillment of the Requirements for the Degree

Master of Chemistry

by

Richard Howell

November, 2013

Oxidation of Isoprene to Methyl vinyl ketone and Methacrolein via Hydroxyl Radical: A Regenerative Mechanism for the Hydroxyl Radical
by

Richard Howell

APPROVED BY:

DIRECTOR OF
DISSERTATION/THESIS: _____
(Libero Bartolotti, PhD)

COMMITTEE MEMBER: _____
(Mary Farwell, PhD)

COMMITTEE MEMBER:_____
(Brian Love, PhD)

COMMITTEE MEMBER: _____
(Yumin Li, PhD)

CHAIR OF THE DEPARTMENT
OF CHEMISTRY:_____
(Rickey Hicks, PhD)

DEAN OF THE
GRADUATE SCHOOL:_____
Paul J. Gemperline, PhD

TABLE OF CONTENTS

LIST OF TABLES

LIST OF FIGURES

List of Abbreviations

VOC: Volatile organic chemical

MVK: Methyl vinyl ketone

MACR: Methacrolein

GABRIEL: Guyanas Atmosphere-Biosphere exchange and Radicals Intensive Experiment with the Learjet

Tg: Teragram = $1x10^{12}$ grams

h: Planck's constant

m: mass

ψ: is the wavefunction

E: total energy

TS: Transition State

MESMER: Master Equation Solver for Multi-Energy Well Reactions

DFT: Density functional theory

HF: Hartree-Fock

$\overline{\nabla}$: Vector differential operator

P: Density

Φ: Kohn-Shame orbital

RRKM: Rice–Ramsperger–Kassel–Marcus

TST: Transition state theory

$\hat{\tau}_i$: Tangential unit vector

$\varepsilon_{i:}$ Lagrange multiplier

Θ: Vector of steepest descent

φ: Angle of rotation

Kcal/mol: kilocalories/mole

kJ/mol: Kilojoules/mole

Å: angstrom = $1x10^{-10}$ m

Chapter 1 Introduction

Introduction

Atmospheric chemistry affects every air breathing creature on this planet. It can be easy to forget that chemical reactions take place not only in labs and factories, but also in the very air surrounding those labs and factories and everything else on the planet. Despite the high level of importance and the sheer magnitude of impact, there are still many reactions that occur in the atmosphere that are not fully understood. Isoprene and the hydroxyl radical are just two examples of molecules involved in atmospheric chemistry. Isoprene and the hydroxyl radical both react with many different classes of molecules in the atmosphere, helping to reduce the levels of these species and in a sense clean the air. In the air above the Amazonian forest, hydroxyl radical was found in concentrations well above levels predicted by computer models.(Eerdekens et al., 2009) To explain these results, the Peeters' group proposed a several different reaction pathways involving isoprene and the hydroxyl radical.(Peeters, Nguyen, & Vereecken, 2009) One of these pathways will regenerate the hydroxyl radical via a 1,5-H shift mechanism.

Background

Isoprene

Isoprene, or 2-methyl-1,3-butadiene, is a five carbon molecule with two double bonds. Isoprene plays an important role in many oxidation reactions in the atmosphere, reacting with many commonly found airborne oxidants including NO_x, OH, and O_3. Isoprene's reactivity with many oxidizing radicals in the atmosphere makes it an

important sink for these species, and is partly responsible for keeping the levels of these highly reactive species in check. Isoprene is available in great quantities in the atmosphere, with approximately 500 Tg of isoprene emitted yearly.(Peeters et al., 2009) Isoprene belongs to a class of molecules known as volatile organic compounds or VOCs.

OH

OH is a molecule comprised of an oxygen atom and a hydrogen atom. In the atmosphere it usually exists in a free radical state and plays an important role in initiating many oxidation reactions with VOCs.(Vereecken & Francisco, 2012) Because it readily reacts with VOCs in the atmosphere, it plays a key role in the life cycle of VOCs, making its origins and sinks of interest in atmospheric chemistry. A free radical is a chemical species that possess an unpaired electron. This lone electron is responsible for the high degree of reactivity and thus for its role as a reaction initiator.

Isoprene + OH

As mentioned previously, the relationship between isoprene and the OH radical is one of reactant and initiator. In these oxidation reactions the hydroxyl radical, along with the VOC it helped oxidize, is generally consumed in the formation of whichever products the two species end up being. In 2005 a project to measure the concentration of isoprene and species relevant to the oxidation of isoprene was conducted over an

area above the northern part of the Amazonian rain forest in a project known as Guyanas Atmosphere-Biosphere exchange and Radicals Intensive Experiment with the Learjet or GABRIEL. The results of the study found that while isoprene and methacrolein(MACR) and methyl vinyl ketone(MVK) were found in expected concentrations, the OH radical was found in far greater amounts than had been predicted.(Eerdekens et al., 2009)

Chapter 2 Theory

Quantum mechanics

In the early part of the 20th century, the work of several physicists gave rise to a field known as quantum mechanics. Of the many advancements to come from their work, perhaps the most important one is the Schrödinger equation. Below is Schrödinger's time independent equation for a one dimensional particle

$$-\left(\frac{h^2}{2m}\right)\frac{(d^2\psi)}{(d^2x)}+V(x)\psi=E\psi \tag{2.1}$$

where h is Planck's constant, m is the mass of the particle, ψ is the wavefunction, V(x) is the potential energy of the particle and E is the total energy of the particle.(Atkins & De Paula, 2006) Even today the Schrödinger equation can only be solved exactly for one electron systems, however, many advances in computers and approximate techniques can be used to solve the Schrödinger equation with a relatively high degree of fidelity.

Computational chemistry

Computational calculations can be split into two categories, empirical and *ab initio*. Empirical calculations rely on data that has been taken from experimental results and used to build a model to describe chemical systems. Like most methods that

involve extrapolation, the accuracy of the results generated by an empirical calculation decrease as the similarity between the system and the data set decrease. *Ab initio* calculations on the other hand are accurate for a wider variety of systems as the results it generates come from solving the Schrödinger's equation as opposed to a data set. To better understand ab initio, consider the Schrödinger equation.

$$\hat{H}\psi = E\psi \tag{2.2}$$

In this general form of the Schrödinger equation, H is an operator, that is it alters the wavefunction psi to give back the same wave function times the energy of the system E. The Hamiltonian $\hat{H}$ accounts for energy contributions due to: nuclear potential energy, electron potential energy, nuclear-electron interactions, electron-electron interactions, and nuclear-nuclear interactions.

$$H = T_n + H_e + H_{mp} \tag{2.3}$$

$$H_e = T_n + V_{ne} + V_{ee} + V_{nn} \tag{2.4}$$

$$H_{mp} = -\frac{1}{2M_{tot}}\left(\sum_{i}^{N_{elec}} \nabla_i\right)^2 \tag{2.5}$$

The Born-Oppenheimer approximation is used to simplify the Hamiltonian to something more manageable as seen in equation 2.3 as opposed to the complete Hamiltonian which consists of many more terms. The Born-Oppenheimer approximation simplifies the Hamiltonian by assuming nuclear $\bar{\nabla}$ or $\bar{\nabla}^2$ operators equal zero when operating on an electronic wave function.(Cramer, 2005) The electronic wave function is built from equations representing molecular orbitals which are constructed from mathematical representations of atomic orbitals found in a basis set.

Basis set

The basis set can be thought of as simply a mathematical description of an atomic orbital. A linear combination of these orbitals is what is used to construct the wave function.(Cramer, 2005) There are many different types of basis sets, each fine-tuned to study a specific set of characteristics or properties.

A basis set is a set of functions which describes the atomic orbitals for a set of atoms. The equations or primitives used to describe these orbitals come in two forms, slater type and Gaussian type orbitals.(Jensen, 2006) Gaussian type orbitals take the following form.

$$\chi_{\zeta,l_x,l_y,l_z}(x,y,z)=Nx^{l_x}y^{l_y}z^{l_z}e^{-\zeta r^2} \quad (2.6)$$

In equation 2.4,N is a normalization constant, ζ is a width controlling exponent, l_x,l_y, and l_z are values whose sum determines the type of orbital, and x,y, and z are Cartesian coordinates.(Cramer, 2005; Jensen, 2006)

Adequately describing the atomic orbitals for each atom requires a significant number of equations, depending on the basis set. Chemical interactions usually only occur in the valence orbitals of an atom, leaving the inner orbitals and electrons untouched. Since solving these equations is computationally intensive, basis sets are often contracted, that is, their inner orbitals are reduced to a linear sum of primitives.(Jensen, 2006)

The basis sets used in this study are the 6-311++G** and the maug-cc-pvtz basis sets. The 6-311++G** basis set belongs to a family of basis sets known as the Pople basis sets. The 6-311++G** is a triple split valence basis set, that is, the valence orbitals are defined by three equations.(Jensen, 2006) The ++ and ** indicates that a diffuse s- and p-functions are included, and that d and p polarization functions have been added respectively. The six refers to the number of contracted primitives used to describe the core orbitals.

The other basis set used is the maug-cc-PVTZ basis set. The original aug-cc-PVTZ basis set, developed by the Dunning group, is a correlation consistent basis set suitable for many first row atoms.(Dunning, 1989) The maug-cc-PVTZ is a modified version of the aug-cc-PVTZ basis set. The Truhlar group removed extraneous diffuse functions for all atoms in the Dunning basis set without sacrificing accuracy and improved the computational cost significantly.(Papajak & Truhlar, 2010) PVTZ in this

case stands for polarized valence triple zeta. Zeta refers to the number of contracted functions used to describe an orbital, in this case, triple zeta would mean three times as many functions are used to describe a single orbital as a single zeta basis set would.

Density functional theory

Traditional *ab initio* calculations rely on constructing the wave function from equations contained within a basis set. As the size of the system being studied increases, the number of calculations required increases as well. Density functional theory ideally would only depend on the electron density and would thus be a three variable problem as opposed to a 4N variable problem with the wave function approach.(Jensen, 2006) unfortunately relying solely on density in a uniform electron cloud model produces results far too inaccurate to be of use in computational chemistry. The work of Kohn and Sham correct this by reintroducing orbitals, at the cost of increasing the complexity from 3 to 3N.(Kohn & Sham, 1965)

$$\delta\{ T_s[\{\Phi_i\}+J[\rho\,]+E_{xc}[\rho\,]+V_{ne}[\rho\,,\nu\,]- \sum_{i=1}^{N} \varepsilon_i\,(<\Phi_i|\Phi_i> - 1)=0 \tag{2.7}$$

$$T_s[\{\Phi_i\}] = -\frac{1}{2}\sum_{i=1}^{N} <\Phi_i|\nabla^2|\Phi_i> \tag{2.8}$$

$$J[\rho] = \frac{1}{2} \iint \frac{\rho(\vec{r})\rho(\vec{r}')}{|\vec{r}-\vec{r}'|} d\tau \, d\tau'$$

(2.9)

$$V_{ne}[\rho] = \int \rho(\vec{r}) v_{ne}(\vec{r}) \, d\tau$$

(2.10)

$$\rho(\vec{r}) = \sum_{i=1}^{N} n_i |\Phi_i|^2$$

(2.11)

Equation 2.5 is a statement of the Kohn-Sham variational principle, where equation 2.6 defines T_s, which is the kinetic energy term for a system of non-interacting electrons, equation 2.7 defines J, which is simply the Coulomb energy, equation 2.8 defines the potential energy for nuclear-electron interactions, E_{xc} is the exchange correlation energy for both potential and kinetic parts, and ρ is the ground state electron density, where n_i is the occupation number of the ith orbital, Φ_i is the ith Kohn-Sham orbital, ε_i is the Lagrange multiplier that ensures the Kohn-Sham orbitals are orthonormal. The Kohn-Sham variational principle is what leads to equation 2.10.

$$-\frac{1}{2}\nabla^2\Phi_i + v_{eff}\Phi_i = \varepsilon_i\Phi_i$$

(2.12)

$$v_{eff} = \frac{\delta J}{\delta \rho} + \frac{\delta E_{xc}}{\delta \rho} + v_{ne}$$

(2.13)

In equation 2.10, ν_{eff}, the effective potential, is defined by equation 2.11, whose terms have been previously explained. Equation 2.10 is analogous to equation 2.2, which is the form used in the wave function approach and will yield the ground state density in theory. E_{xc} may be defined different for different implementations of DFT. In the M062X functional developed by Truhlar, the exchange functional is defined below.(Zhao & Truhlar, 2008)

$$E_{XC}^{hyb} = \frac{X}{100} E_X^{HF} + \left(1 - \frac{X}{100}\right) E_X^{DFT} + E_C^{DFT} \tag{2.14}$$

Equation 2.14 is the exchange correlation term for the M062X functional, where X is the percentage of Hartree-Fock exchange, E_X^{HF} is the exchange energy for Hartree-Fock, E_X^{DFT} is the exchange energy for DFT, and E_C^{DFT} is the correlation energy for DFT. The E_X^{DFT} depends on the local spin density and the exchange energy density. The DFT correlation energy E_C^{DFT} depends on the reduced spin density, which is derived from the spin density.

Kinetics

Kinetics deals with rates, rates of formation and rates loss. Since kinetics deals with rates of change it naturally comes in the form of differential equations.

$$\frac{d[B]}{dt} = -\frac{d[A]}{dt} \tag{2.15}$$

Equation 2.12 expresses the relationship between the rate of change in concentration of reactant [A] as it forms product [B] for a chemical reaction A → B. This rate of change depends on some constant k and usually depends on the concentration of the reactants raised to some power depending on the reaction.

$$\frac{d[A]}{dt} = -k[A] \tag{2.16}$$

This constant k can be related to the energy of activation by the Arrhenius equation.(Atkins & De Paula, 2006)

$$\ln k = \ln A - \frac{E_a}{RT} \tag{2.17}$$

In the Arrhenius equation, k is a rate constant, A is a pre-exponential factor, E_a is the energy of activation, R is the ideal gas constant, and T is the temperature.(Atkins & De Paula, 2006) The energy of activation is simply the energy barrier on a reaction pathway going from reactants to products, which can also be thought of as the energy difference between the reactants and the transition state that lies between the two. The transition state is a maxima on the potential energy surface that lies between reactants and products.

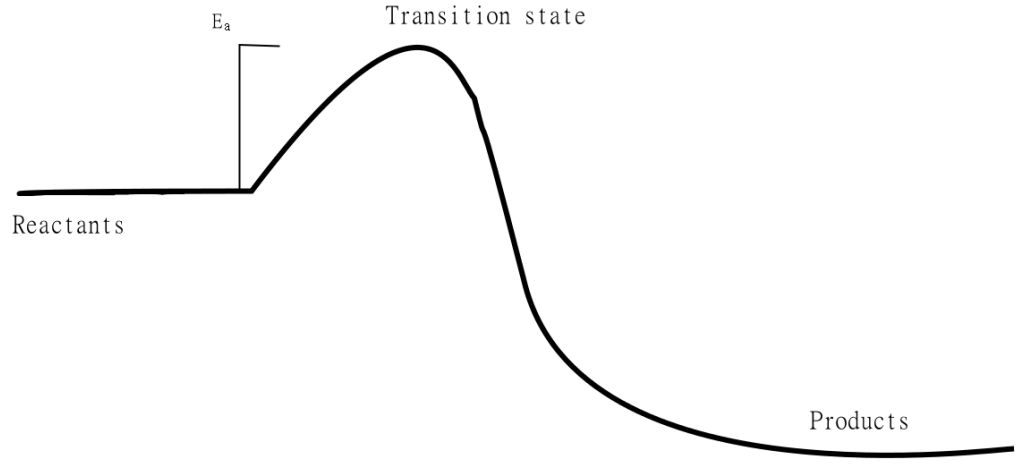

Figure 2.1: Simple energy pathway

This forms the foundation for transition-state theory. Transition-state theory relates the energy of activation as well as the Gibbs energy of activation to the rate constant. This approach is useful for some systems, but it does have its limitations. Transition-state theory assumes that the reacting molecules are in thermal equilibrium with the environment which is not necessarily the case for gas phase reactions.(Jensen, 2006)

The master equation approach attempts to remedies these shortcomings by including terms to account for collisional energy and is based on RRKM models rather than TST.(Glowacki, Liang, Morley, Pilling, & Robertson, 2012; 2012) The master equation lends itself well to matrix solutions. The master equation, which is normally in the form of a coupled set of differential equations, may be expressed in matrix form depicted below.

$$\frac{d}{dt}p=Mp$$

(2.18)

In equation 2.17, p is a vector which contains the population densities and M is the transition matrix which was constructed from the master equation.

NEB

The nudged elastic band (NEB) is a method for mapping out the reaction pathway between two points on a potential energy surface.(Sheppard, Terrell, & Henkelman, 2008)(Jónsson, Mills, & Jacobsen, 1998) Points along the reaction pathway are generated in one of several different ways, usually a direct linear interpolation between the two points being the easiest and most straight forward.

$$F_i^{NEB}=F_i^{\perp}+F_i^{||}$$

(2.19)

$$F_i^{\perp}=\nabla(R_i)+\nabla(R_i)\cdot\hat{\tau}_i\hat{\tau}_i$$

(2.20)

$$F_i^{||}=k(|R_{i+1}-R_i|-|R_i-R_{i-1}|)\hat{\tau}_i$$

(2.21)

F_i^{NEB} is the total force acting on point i in the NEB, $F_i^{\perp}$ is the perpendicular force, R_i is the is the position of the ith point, $\hat{\tau}_i$ is the tangential vector that points towards the neighboring point with the highest energy, $F_i^{||}$ is the parallel force, and k is the spring constant. The force parallel is responsible keeping the points equidistant from each other. The perpendicular force is responsible for moving the points down the potential energy gradient. The perpendicular force may be modeled by one of many different optimization algorithms available.

DIMER

The dimer method, developed by Hinkelman, is a method for finding transition states using only gradients.(Heyden, Bell, & Keil, 2005) Two points, R_1 and R_2, on the reaction pathway are selected as the starting points for the dimer optimization method. A third point, R_0, between the two given points is chosen. A unit vector N derived from the vector connecting the two starting points is then rotated to the lowest curvature mode with respect to the energy at the point R_0.

$$C_N = \frac{E_1 + E_2 - 2E_0}{\Delta R^2} \tag{2.22}$$

The curvature is then calculated for the vector N by equation 2.15, where C_N is the curvature, E_1,E_2, and E_0 is the energy for R_1,R_2, and R_0 respectively, and ΔR is the distance between R_0 and R_1. To locate the appropriate step direction, the direction of steepest descent, the follow equation is used.

$$\frac{\partial E}{\partial \varphi} = -\Delta R(F_1 - F_2)^T \Theta$$

(2.23)

In equation 2.16, F_1 and F_2 are the forces acting upon R_1 and R_2 respectively, φ is the angle of rotation, and Θ is the vector of steepest descent. The appropriate angle of rotation can be determined from the following equation.

$$\varphi_{min} = -\frac{1}{2}\arctan\left(\frac{2F}{F'}\right) - \frac{\delta\varphi}{2}$$

(2.24)

$$F = \frac{([(f_1 - f_2)^T \cdot \Theta]_{\phi=\delta\varphi} + [(f_1 - f_2)^T \cdot \Theta]_{\phi=0})}{2}$$

(2.25)

$$F' = \frac{([(f_1 - f_2)^T \cdot \Theta]_{\phi=\delta\varphi} - [(f_1 - f_2)^T \cdot \Theta]_{\phi=0})}{\delta\varphi}$$

(2.26)

Equation 2.17 describes the angle of rotation for the direction of minimal curvature, where F is the rotation force, and F' is the curvature force, and f_1 and f_2 have are the forces acting upon R_1 and R_2. Next the dimer midpoint R_0 is translated along a force vector $f^{\dagger}$ which is calculated from the following equation.

$$f^{\dagger}=\begin{cases} -\left(f_0^T\cdot N\right)N \text{ if } C_N>0 \\ f_0-2\left(f_0^T\cdot N\right)N \text{ if } C_N<0 \end{cases}$$

(2.27)

$$\Delta x=-\frac{\left(f^{\dagger}\big|_{x=\delta x}+f^{\dagger}\big|_{x=0}\right)^T\cdot\frac{N^{\dagger}}{2}}{\left(f^{\dagger}\big|_{x=\delta x}-f^{\dagger}\big|_{x=0}\right)^T\cdot\frac{N^{\dagger}}{\delta x}}+\frac{\delta x}{2}$$

(2.28)

Next the length of the step to take is calculate from equation 2.21, where $N^{\dagger}$ is the normal vector along the vector $f^{\dagger}$.

Chapter 3

Results

Each overall reaction was modeled in two pieces, isoprene/OH/O_2 complexed going to the appropriate isoprene-OH-O_2 adduct and from the isoprene-OH-O_2 adduct going to the appropriate products. The M062X density functional was used in all calculations except for those done by MESMER.

Minimizing the structures

The initial structures for all species in this study were first modeled in the software modeling package Material Studios.(Accelrys Software Inc, 2008) The structures are refined to the point of bond lengths and angles being set to ideal theoretical values. This makes a good starting point for the minimization process, but is too inaccurate to be used directly for quantitative values. The generated structures are then fed into the Gaussian 09 software package.(Frisch et al.,) Gaussian 09 is a quantum mechanical software package with support for many different levels of theory as well as different basis sets. The structures are initially optimized at the M062X density functional level of theory using the 6-311++G** basis set. Care was taken to ensure that the minimized structures chosen for the next step of the study were the lowest energy structures possible.

Constructing the NEB

For each piece of the NEB, the starting point(reactants) and the end point(products) needed to be minimized to produce good results. Each NEB calculation was run with a total of 31 images, or points along an NEB pathway, until the desired features were identifiable and refined enough for further optimization. Special care was taken in the course of these calculations to ensure the energy pathway the NEB was following was the lowest energy pathway for the ground state of the species involved.

Anti-MVK

The information generated by the NEB and from the final minimization of the wells and transition states were used to construct Figure 3.1. The species and energies in kcal/mol have been labeled on the figure.

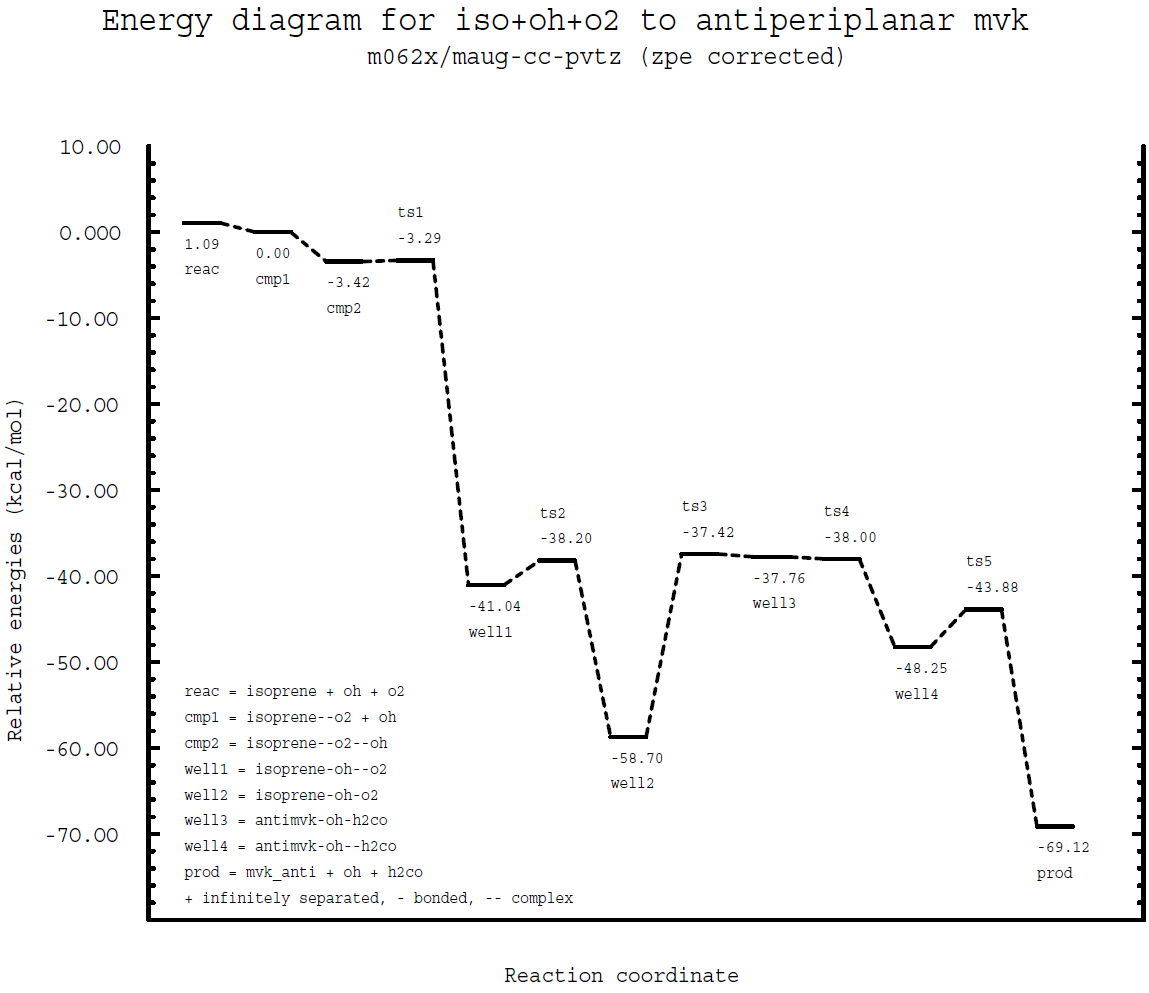

Figure 3.1: ZPE corrected energy diagram for antiperiplanar MVK

The mechanism starts with all three reactants infinitely separated. O_2 then forms a complex with isoprene, pictured below in Figure 3.2.

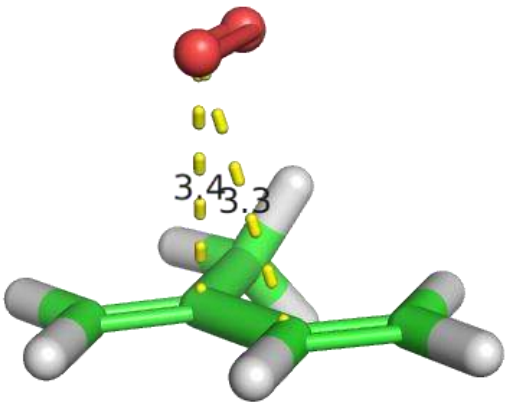

Figure 3.2: Isoprene/O_2 complex

There is a very slight decrease in energy in forming this complex. The oxygen molecule is interacting with both double bonds on the isoprene molecule at around 3.3 Å. From this point the hydroxyl radical then approaches the isoprene/O_2 complex near the 1 carbon.

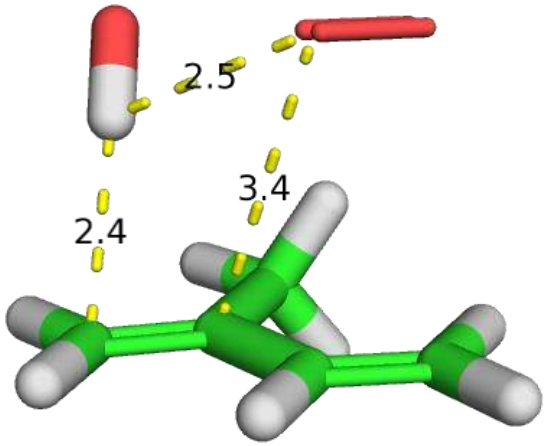

Figure 3.3: Isoprene/OH/O_2 complex

In the resulting complex that is formed shown in Figure 3.3, the hydroxyl radical takes up a position directly above the 1 position in the isoprene at 2.4 Å. The O_2 molecule has been pushed slightly away from its original position straddling the two pi bonds in isoprene. Additionally, the oxygen molecule has rotated itself slightly due to hydrogen interactions between the oxygen molecule and the hydrogen on the hydroxyl radical. From here the hydroxyl radical can begin the oxidation of the isoprene by reacting with the 1 carbon in the isoprene molecule.

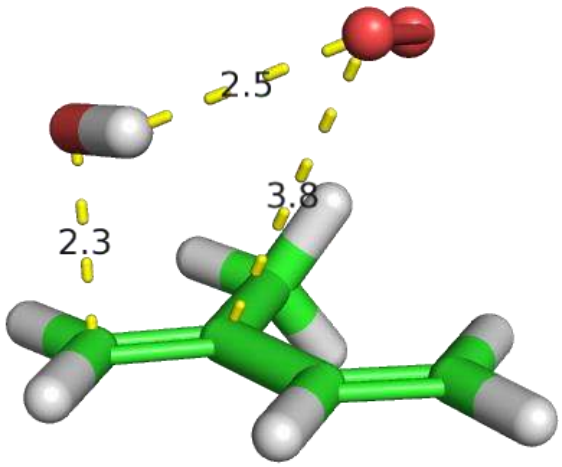

Figure 3.4: MVK TS1

The first transition state is for the bond formation between the 1 position of isoprene and the hydroxyl radical. The hydroxyl radical has rotated from its earlier orientation in the complex to allow for the radical to interact with the 1-2 pi bond and ultimately bond with the isoprene molecule. Oxygen has been pushed out of the way for this stage of the reaction, nearly 0.5 Å farther from the 2 carbon than earlier. The oxygen has however maintained a 2.5 Å distance from the hydroxyl radical, indicating that the hydrogen interactions are strong than the interaction between oxygen and the pi bonds in isoprene.

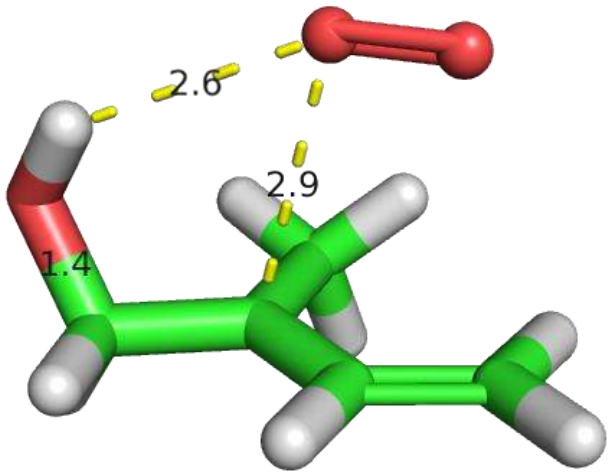

Figure 3.5: Isoprene-OH adduct complexed with O_2

Going through the first transition state, the hydroxyl radical has now added to the 1 position of the isoprene molecule, forming 1-hydroxy-2-methyl-3-butene radical. The radical center, now located on the 2 carbon, is stabilized by the presence of the methyl group and also to a lesser extent by delocalization through the pi system at the 3-4 carbons. The oxygen molecule is now once again located above the 2 carbon, which is now the radical center and sets the stage for the next step in the mechanism.

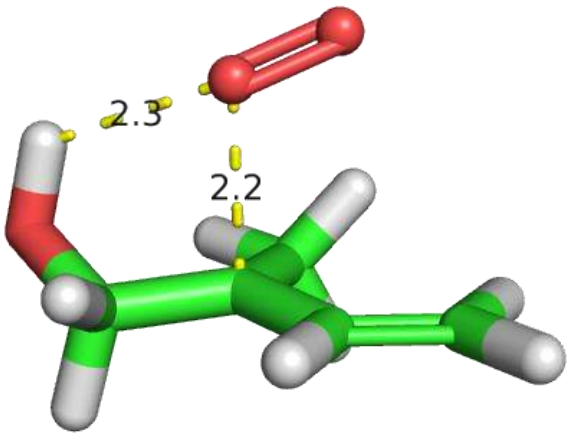

Figure 3.6: MVK TS2

In the second transition state, the oxygen approaches the radical center on the 2 position of the isoprene-OH adduct. The hydrogen interactions between the 1-OH group and the oxygen molecule assist in guiding the oxygen to the 2 carbon.

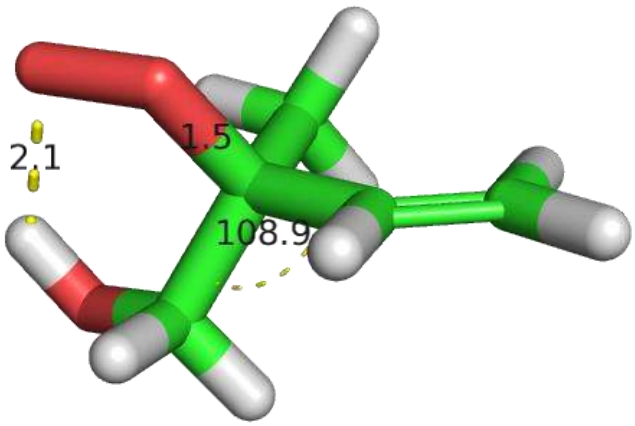

Figure 3.7: Anti-isoprene-OH-O_2 adduct

The addition of oxygen at the 2 carbon gives the anti-conformation of the isoprene-OH-O_2 adduct, or anti-1-hydroxy-2-peroxy-3-butene radical. The radical center is now located on the second oxygen atom of the peroxy group located on the 2 carbon. The 2 carbon has now assumed a tetrahedral geometry due to the free radical being replaced by a proper bond with a carbon-carbon bond angle of 108.9°. The radical center on the oxygen now has a stronger hydrogen interaction with hydrogen located on the 1-hydroxy group. This strong interaction hints at the upcoming 1,5 hydrogen shift.

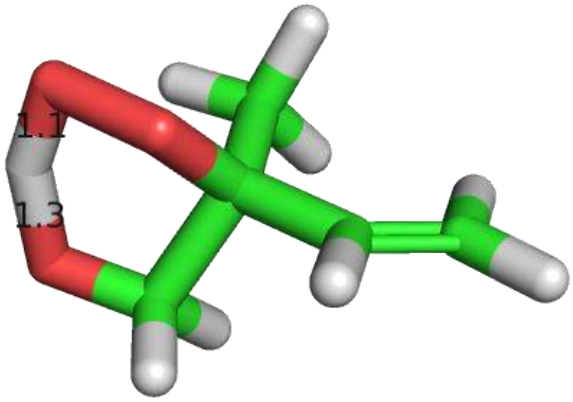

Figure 3.8: Anti-MVK TS3

The third transition state is for the 1,5-H shift. Here the hydrogen is located between the two oxygens, favoring the oxygen on the 2 peroxy group slightly by 0.2 Å.

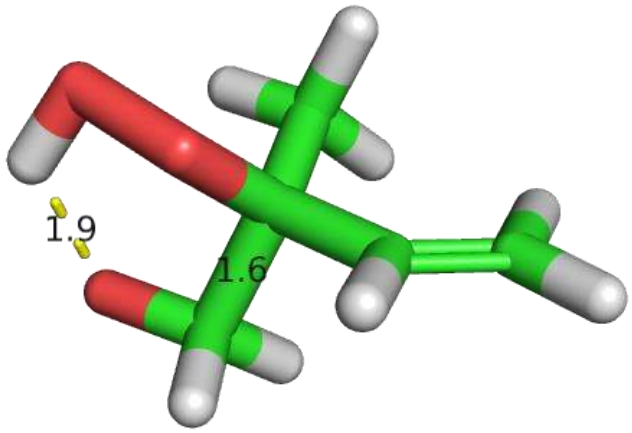

Figure 3.9: Isoprene/O/O_2H molecule

After the third transition state, the molecule in Figure 3.9 is formed. 1-oxy-2-perhydroxy-2-methyl-3-butene now has the free radical located on the oxygen atom attached to the 1 carbon. The instability caused by the return of the radical to the oxygen atom on the 1 carbon has strained the 1-2 carbon carbon bond, which will break in the upcoming step.

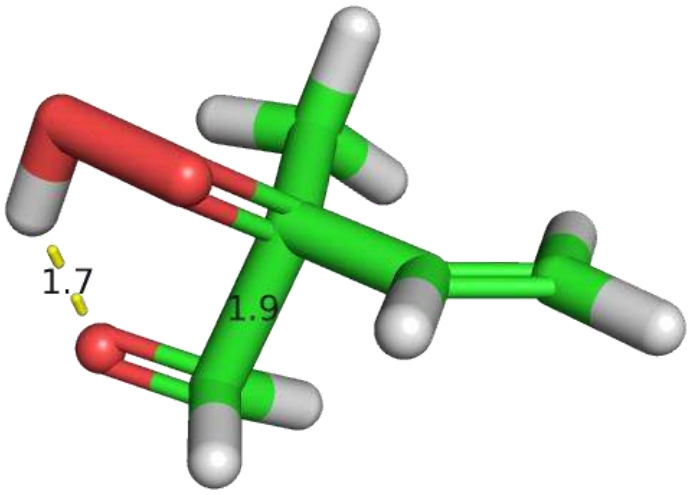

Figure 3.10: Anti-MVK TS4

The fourth transition state is for the breaking of the 1-2 carbon carbon bond. Both carbons 1 and 2 has assumed a trigonal planar like configuration at this point. The hydrogen interactions between the oxygen on carbon 1 and the hydrogen on the hydroperoxy group remain strong.

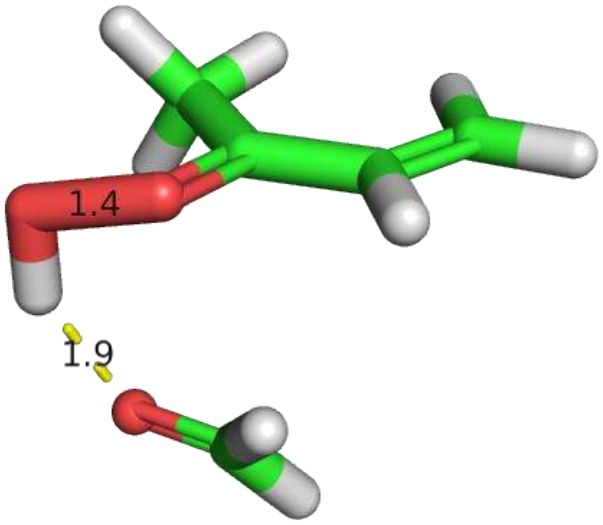

Figure 3.11: 3-perhydroxy-1-butene radical complexed with formaldehyde

The now formaldehyde has completely broken away from the former isoprene molecule and still remains complexed with it due to the hydrogen interactions with the perhydroxy group. The free radical, now centered on the second oxygen in the perhydroxy group, is now destabilizing the oxygen oxygen bond and will ultimately cause a hydroxyl radical to break away.

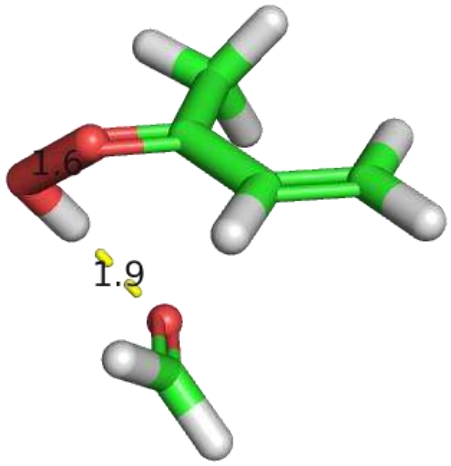

Figure 3.12: Anti-MVK TS5

Figure 3.12 depicts the fifth and final transition state for this mechanism. The formaldehyde is still complexed due to the hydrogen interactions with the perhydroxy group. The hydroxyl radical is breaking away at this point going to the final products. It is at this point the hydroxyl radical is finally regenerated and the oxidation of isoprene to methyl vinyl ketone is complete.

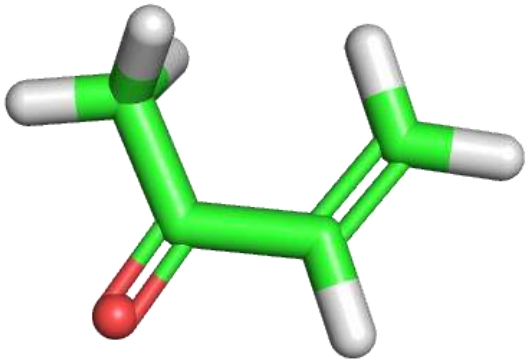

Figure 3.13: Anti-methyl vinyl ketone

Syn-MVK

The mechanism for the oxidation of syn-MVK is very similar to that of anti-MVK, with the first two steps being identical.

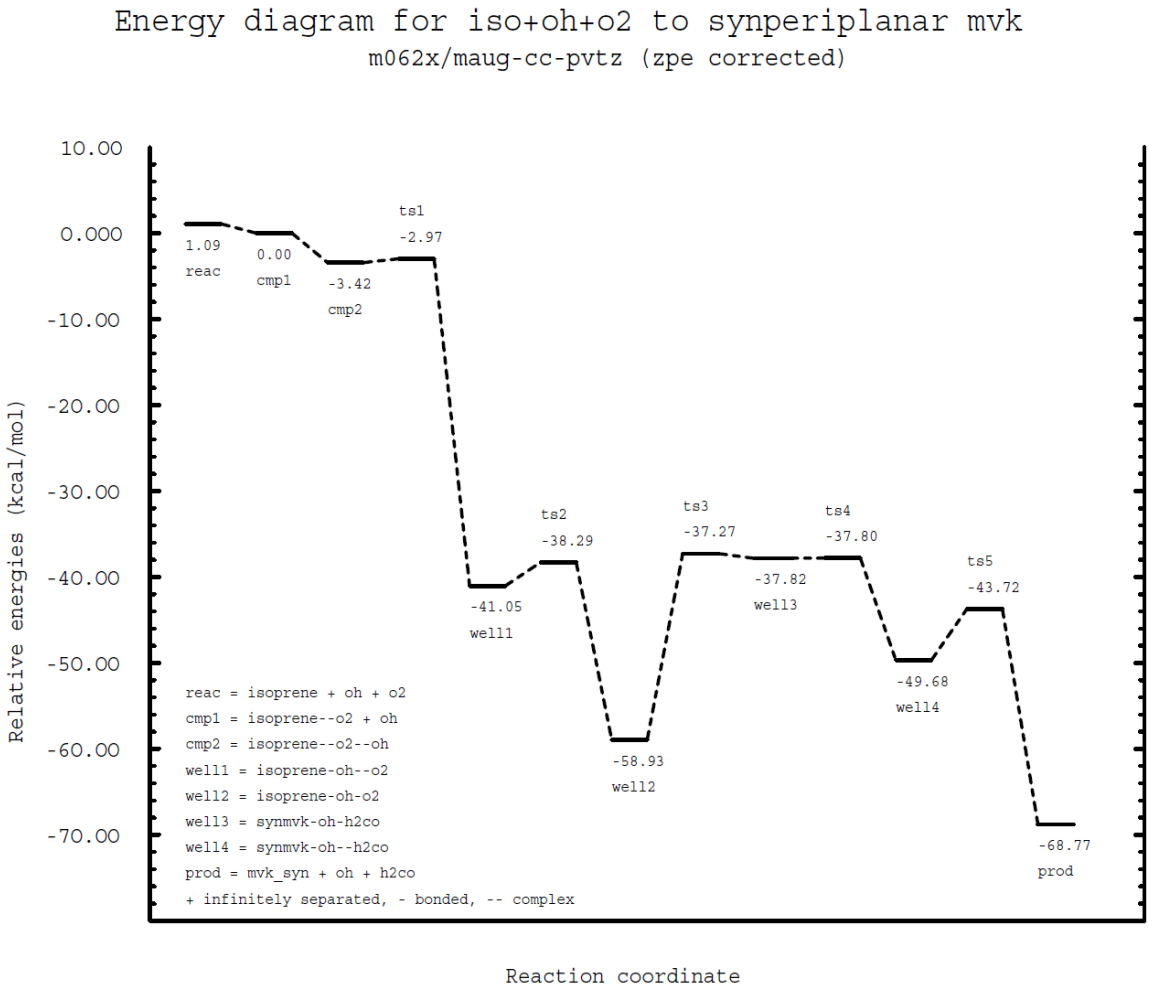

Figure 3.14: Energy diagram for synperiplanar MVK

The mechanism itself proceeds much in the same way as the mechanism for anti-MVK.

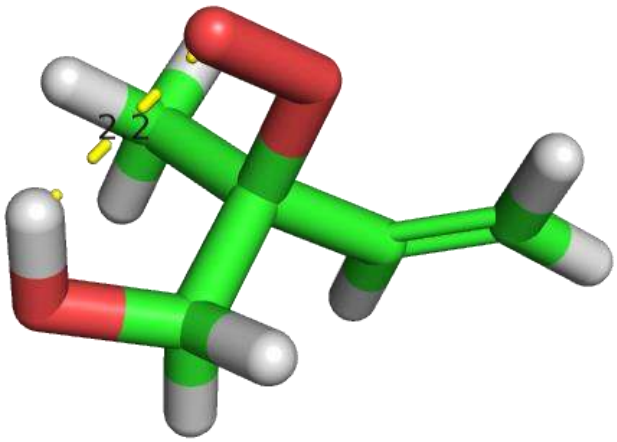

Figure 3.15: Syn-1-OH-2-O_2-isoprene radical

In this adduct the peroxy group and the 3-4 pi bond are now on the same side of the 2-3 carbon bond hence it is syn. As with the analogous anti adduct, the syn version also contains the strong hydrogen interaction between the second oxygen on the peroxy group and the hydrogen on the hydroxyl group. The free radical is located on the second oxygen in the peroxy group as with the anti-analogue.

The mechanism at this point proceeds in much the same way as it did with the anti-version. The hydrogen undergoes a 1,5-H shift over to the peroxy group. Then carbon 1 breaks off to form formaldehyde, leaving the radical on the second oxygen in the perhydroxy group. Finally the oxygen oxygen bond in the perhydroxy group breaks regenerating the hydroxyl radical and forming syn-MVK.

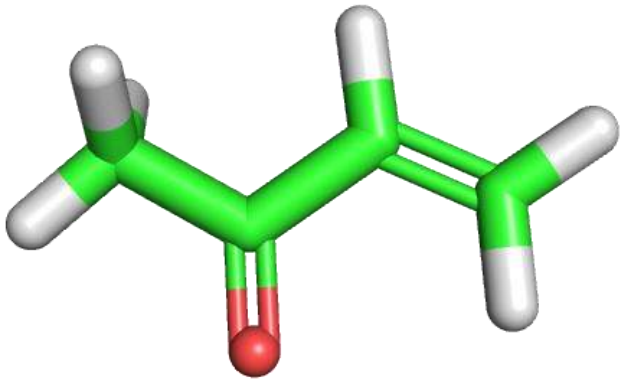

Figure 3.16: Syn-methyl vinyl ketone

Anti-MACR

The oxidation of isoprene to methacrolein is virtually identical from a mechanistic standpoint. Fundamentally, however, it is different in that the reaction takes place at the 3 and 4 carbons instead of carbons 1 and 2 with methyl vinyl ketone.

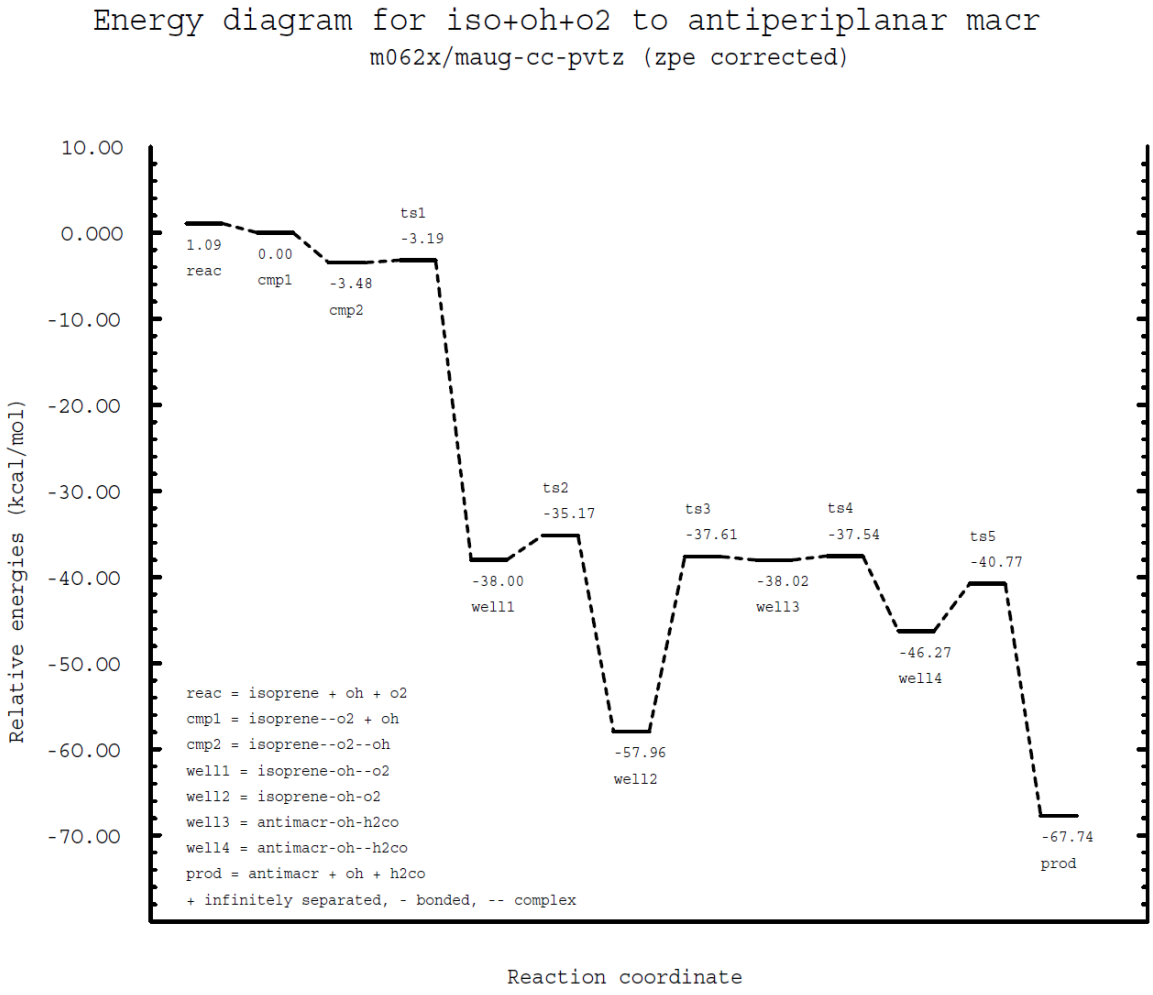

Figure 3.17: Energy diagram for antiperiplanar MACR

The energy diagram for antiperiplanar MACR is very much the same as the energy diagrams for both forms of MVK.

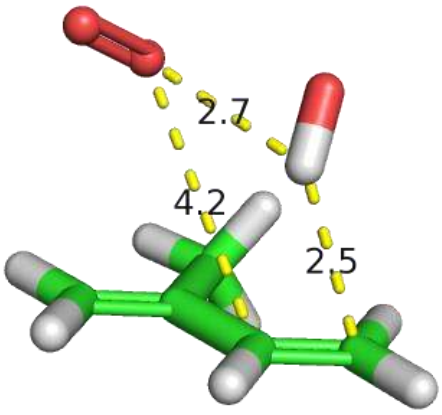

Figure 3.18: Isoprene/OH/O_2 complex for anti MACR

The prereactive complex for MACR is similar to MVK, with the hydrogen on the hydroxyl interacting with both the oxygen molecule and the 3-4 pi bond. Oxygen has also assumed a similar orientation as before, with the only notable difference being that oxygen is now 4.2 Å from the carbon it will ultimately bond with as opposed to 3.4 Å with MVK.

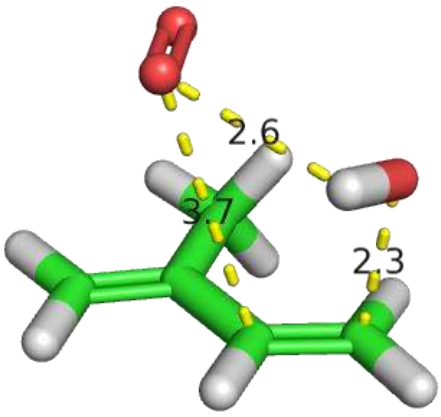

Figure 3.19: MACR TS1

The hydroxyl radical once again initiates the oxidation reaction with isoprene. The hydroxyl radical has rotated into a bonding position about 2.3 Å from carbon 4. Oxygen is still interacting with the hydrogen on the hydroxyl radical at a distance of 2.6 Å. These distances are very similar to those found in the reaction for MVK in Figure 3.4.

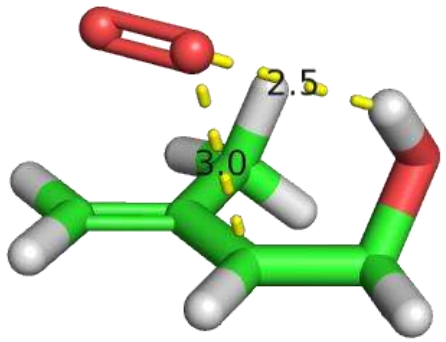

Figure 3.20: 4-hydroxy-2-methyl-1-butene radical complexed with oxygen

The hydrogen interactions between the hydroxyl group and the oxygen molecule help keep the oxygen tethered in place for the next step of the mechanism. A notable difference between the MACR and MVK mechanisms is the oxygen tends to be farther away from isoprene in the MACR complexes than it is in the MVK complexes.

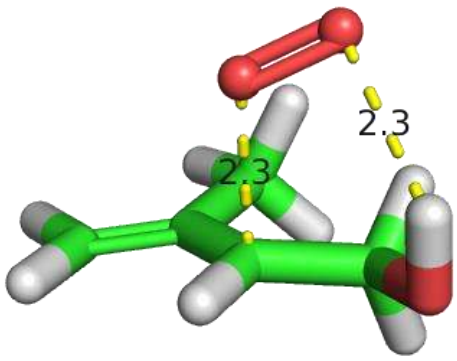

Figure 3.21: Anti-MACR TS2

The second transition state places the oxygen molecule 2.3 Å from both the carbon reactive site and the hydroxyl hydrogen. Unlike the MVK mechanism where the closest oxygen added and then the second oxygen rotated to face the hydroxyl hydrogen, the oxygen atom farthest from the hydroxyl group adds to the 3 carbon in an orientation which positions the non-reacting carbon facing the hydroxyl hydrogen.

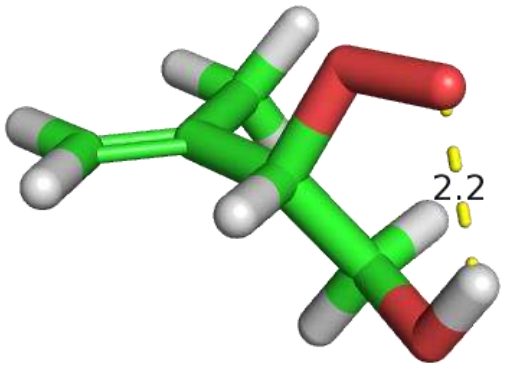

Figure 3.22: Anti-4-hydroxy-3-peroxy-2-methyl-1-butene radical

4-hydroxy-3-peroxy-2-methyl-1-butene is virtually identical to the MVK analogue with the only difference being the location of the peroxy and the hydroxyl groups.

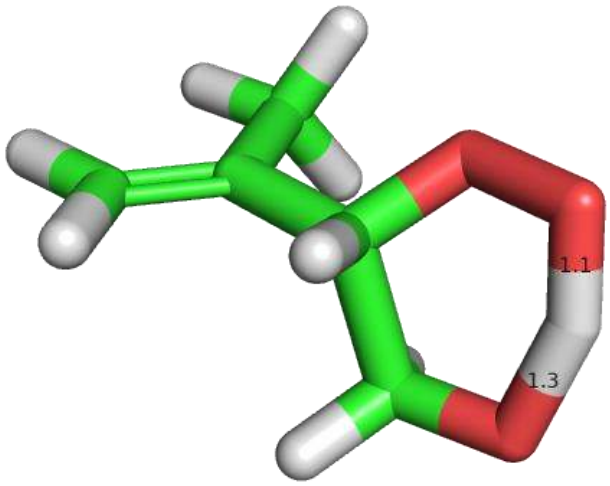

Figure 3.23: Anti-MACR TS3

The transition state for the 1,5-H shift from the hydroxyl group to the peroxy group is very much the same as it was in both MVK reactions.

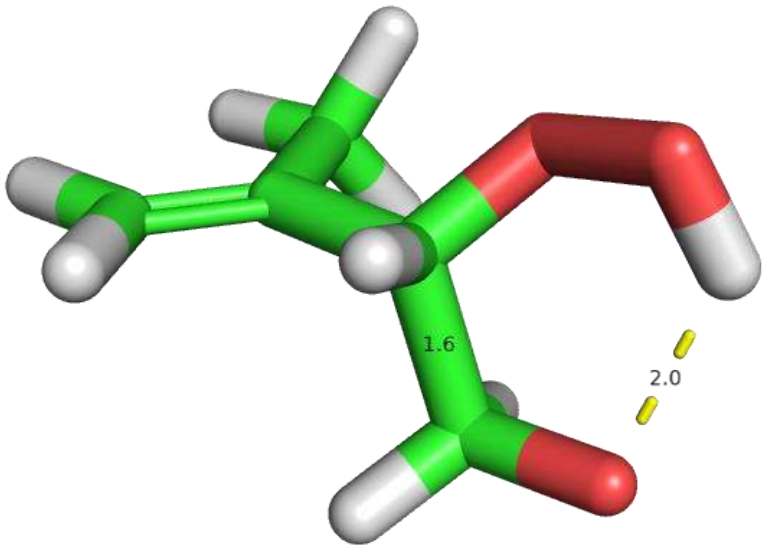

Figure 3.24: Anti-4-oxy-3-perhydroxy-2-methyl-1-butene radical

The intermediate formed after the 1,5-H shift is also virtually identical to the MVK counterpart in terms of bond distances between the oxygen on carbon 4 and the hydrogen on the perhydroxy group, as well as the carbon carbon bond distance between carbons 3 and 4.

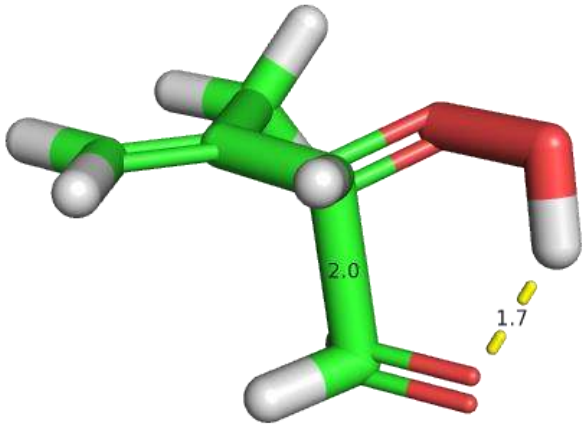

Figure 3.25: Anti-MACR TS4

The fourth transition state for the breaking of the 3-4 carbon carbon bond is again very similar to the MVK analogue. Only a minute difference of 0.1 Å in the carbon carbon bond between isoprene and the leaving formaldehyde exists.

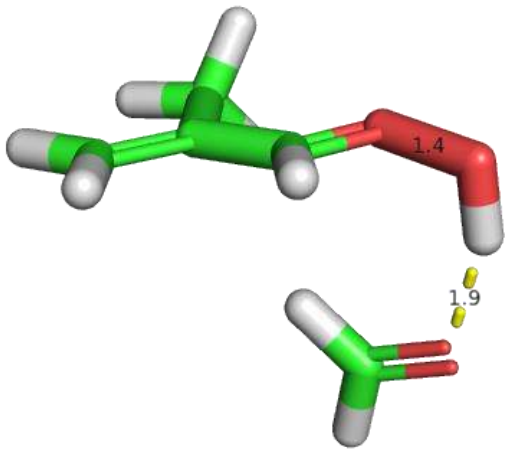

Figure 3.26: Anti-3-perhydroxy-2-methyl-1-propene complexed with formaldehyde

The formaldehyde remains complexed after breaking away from the former isoprene molecule, with hydrogen interactions once again being the governing force at work. The radical, now located on the second oxygen in the perhydroxy group, is destabilizing the group and will facilitate the regeneration of the hydroxyl radical in the upcoming step.

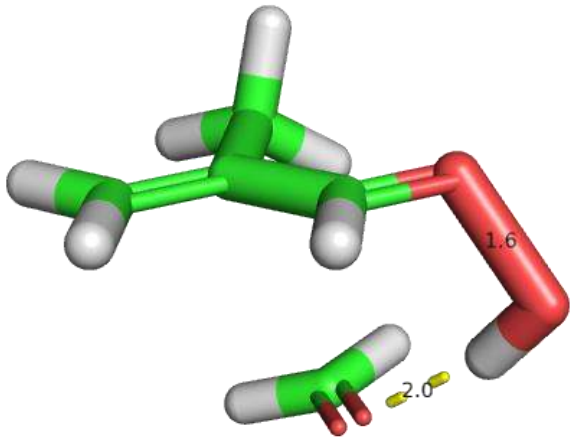

Figure 3.27: Anti-MACR TS5

In this final step the hydroxyl radical is breaking away from the perhydroxy group, leaving the final products of methacrolein, formaldehyde and a hydroxyl radical. One detail to note is the similarity between the position and orientation of the formaldehyde in Figure 3.26 and the orientation of the oxygen molecule in the earlier isoprene complexes.

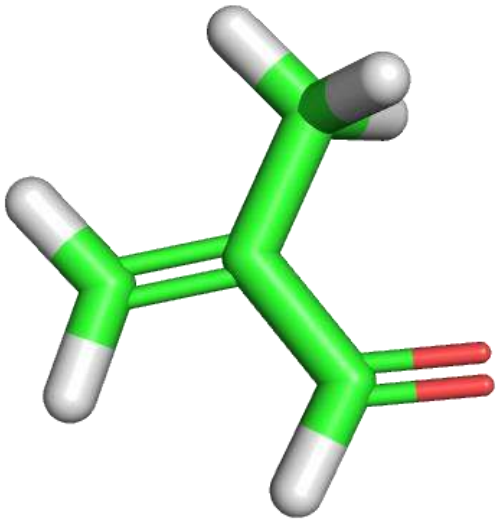

Figure 3.28: Anti-MACR

Syn-MACR

Syn-MACR shares a similar relationship to anti-MACR as the one of syn-MVK to anti-MVK.

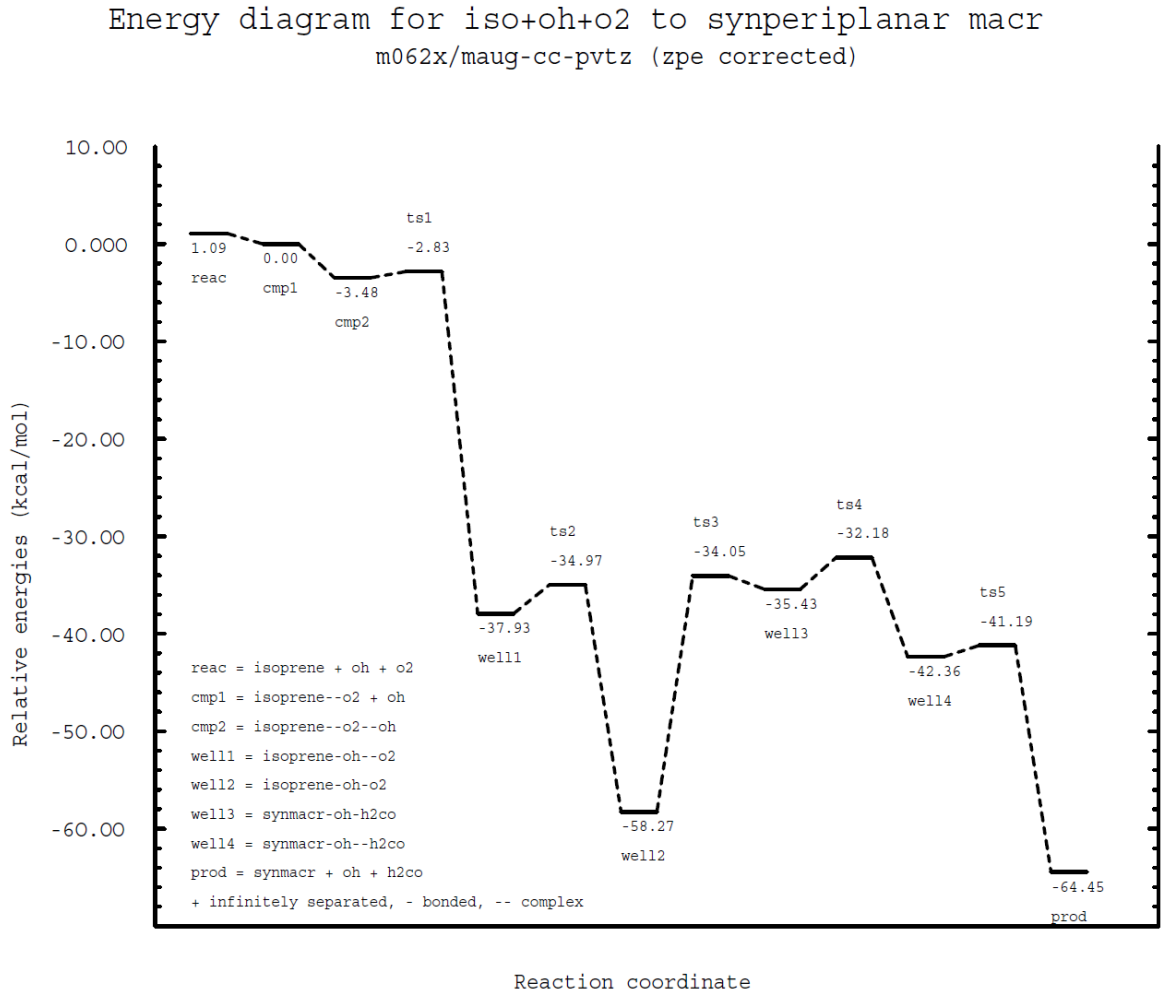

Figure 3.29: Energy diagram for synperiplanar MACR

The energy diagram for the oxidation of isoprene to syn-MACR is similar to that of anti-MACR with the notable difference in energies of TS4.

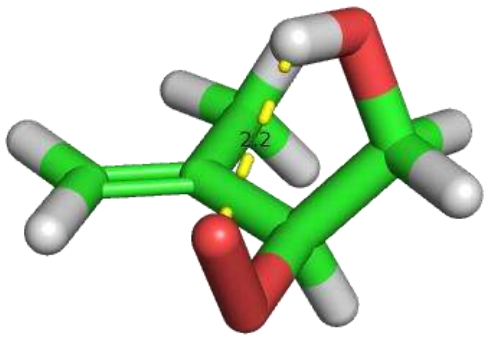

Figure 3.30: Syn-4-hydroxy-3-peroxy-2-methyl-1-butene radical

This is the isoprene/OH/O_2 adduct for syn-MACR. The distinguishing feature is once again the relationship between the carbon carbon double bond between carbons 1 and 2 and the peroxy radical on carbon 3. The reaction proceeds much in the same way as the anti-MACR pathway through the 1,5-H shift and up to TS4.

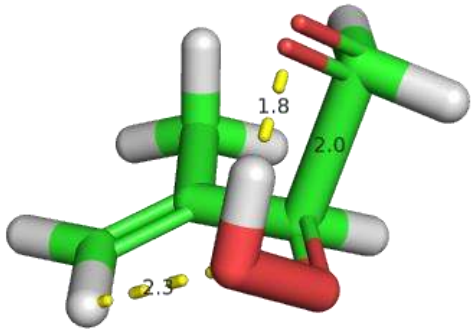

Figure 3.31: Syn-MACR TS4

The fourth transition state is very similar to the anti-MACR counterpart in terms of bond lengths and distances. However, there is one important factor here that wasn't present in any of the other three reaction pathways, steric hindrance between the perhydroxy group and hydrogens on the 1 carbon. This difference is believed to be the cause for the significantly higher energy of this species compared to the species at this step for the other three pathways.

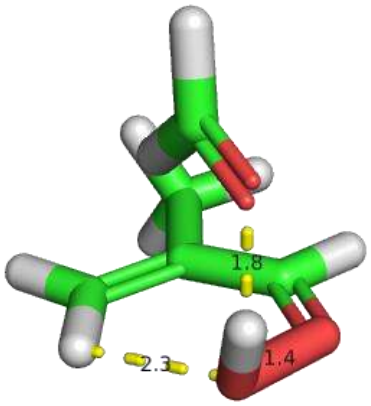

Figure 3.32: Syn-3-perhydroxy-2-methyl-1-propene complexed with formaldehyde

The steric effects between the 1 carbon and the 3 perhydroxy group continue to push the energy several kcal/mol higher than the anti-version of this intermediate. The formaldehyde remains hydrogen bonded to the perhydroxy group as with the anti-analogue.

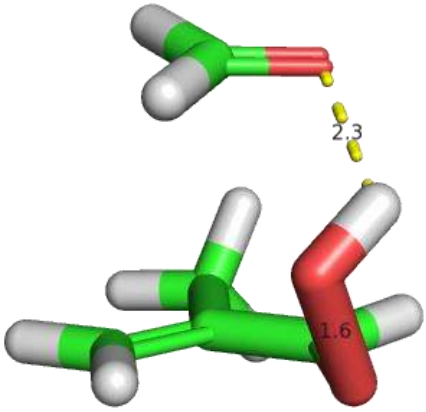

Figure 3.33: Syn-MACR TS5

In the final step of this mechanism the hydroxyl molecule breaks away from the perhydroxy group. With the departure of the hydroxyl radical, the steric effects are reduced, but not completely eliminated. From this point the molecules drift away leaving syn-MACR, formaldehyde and a hydroxyl radical.

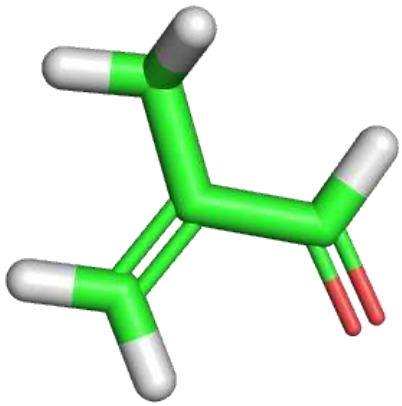

Figure 3.34: Syn-MACR

Further refinement

Once the NEB had adequately resolved the points of interest along the reaction pathway, the appropriate structures were once again fed to Gaussian for minimization. The minimization process is the same as it was for the initial structures, except for the use of the maug-cc-pvtz basis set instead of the 6-311++G**. The maug-cc-pvtz basis set, being larger than the 6-311++G**, provides more accurate results for the energies and geometries at the cost of increased computational time.

DIMER

The transition states were refined using the improved DIMER method. The DIMER method takes two points on a reaction pathway near a transition state and uses the two points to extrapolate a third point. The third point serves as a guess for the transition state and the process is repeated until the optimization parameters are met. The improved DIMER method has an advantage of traditional TS optimization techniques in that is only uses the gradients in its calculations as opposed to second derivatives, which are very costly to calculate.

Frequency

After all minima and transition states have been refined, they are once more fed to the Gaussian software package for frequency calculations. A frequency calculation determines the intensity and wave numbers associated with the 3N-6 different modes of vibration for a molecule. This information is what will be used by the MESMER software package to calculate the kinetics of the reaction as well as the percent yields of each product.

MESMER

MESMER is a software package used for generating kinetic and percent yields for reactions, as well as other data.(Glowacki et al., 2012; 2012) MESMER uses the master equation approach to generate kinetic information, as opposed to traditional

methods like TST and RRKM. MESMER's master equation approach has been shown to provide good results for atmospheric reactions.(Glowacki et al., 2012; 2012)

Kinetics and yields

A frequency calculation was run on each of the minima and transition states for all four reaction pathways. The resulting frequency data along with energies were processed by the MESMER software package to calculate rate constants and product yields.

	Anti MVK (kcal/mol)	**Syn MVK (kcal/mol)**	**Anti MACR (kcal/mol)**	**Syn MACR (kcal/mol)**
Isoprene+OH+O_2	1.09	1.09	1.09	1.09
Complex 1	0.00	0.00	0.00	0.00
Complex 2	-3.42	-3.42	-3.47	-3.47
TS1	-3.22	-3.22	-3.13	-3.13
Well1	-41.05	-41.05	-37.99	-37.99
TS2	-38.15	-38.23	-35.12	-34.90
Well2	-58.69	-58.92	-57.94	-58.28

TS3	-37.37	-37.20	-37.56	-34.00
Well3	-37.75	-37.82	-38.01	-35.43
TS4	-37.94	-37.72	-37.49	-32.11
Well4	-48.24	-49.67	-46.28	-42.36
TS5	-43.82	-43.65	-40.71	-41.17
Product	-80.20	-77.33	-77.09	-75.56

Table 1: ZPE corrected energies for all species in all reactions relative to the energy of isoprene/OH/O_2 prereactive complex in kcal/mol

The energies listed in table 1 are the ZPE corrected energies for all of the species and intermediates. These values can be considered reliable as they match well with work done previously in the literature at a higher level of theory.(Silva, Graham, & Wang, 2009; 2009) The enthalpy of activation for the 1,5-H shift for anti-MVK at 298K 20.8 kcal/mol, compared to 21.8 kcal/mol with G3SX and 20.8 kcal/mol with CBS-QB3 obtained by da Silva.(Silva et al., 2009; 2009) Additionally, the 1,5-H shift's enthalpy of activation for anti-MACR at 298K was calculated as 19.8 kcal/mol, compared to 21.7 kcal/mol with G3SX and 20.7 kcal/mol with CBS-QB3.(Silva et al., 2009; 2009) That values found by da Silva were calculated at a higher level of theory, which suggests the values calculated in this study are accurate even at the lower level of theory. In addition to this, a calculation at the CCSD(T) level of theory with the maug-cc-PVTZ basis set was run on the 1-hydroxy-2-peroxy-2-methyl-3-butene radical and the transition state corresponding to the 1,5-H shift mechanism for the species mentioned earlier and the

energy barrier was found to be 26.3 kcal/mol, compared to the barrier of 25.3 kcal/mol calculated at the M062X level of theory with the maug-cc-PVTZ basis set. All this evidence would support the conclusion that M062X density functional and the maug-cc-PVTZ is suitable for mapping out the mechanisms of atmospheric reactions and in this case provided results which were on par with results generated at a higher level of theory.

For these reactions, it is possible to convert between the syn and anti-forms of either MACR or MVK, depending on the location the hydroxyl radical added to. This possibility was taken into consideration when the yields were calculated by the MESMER program.

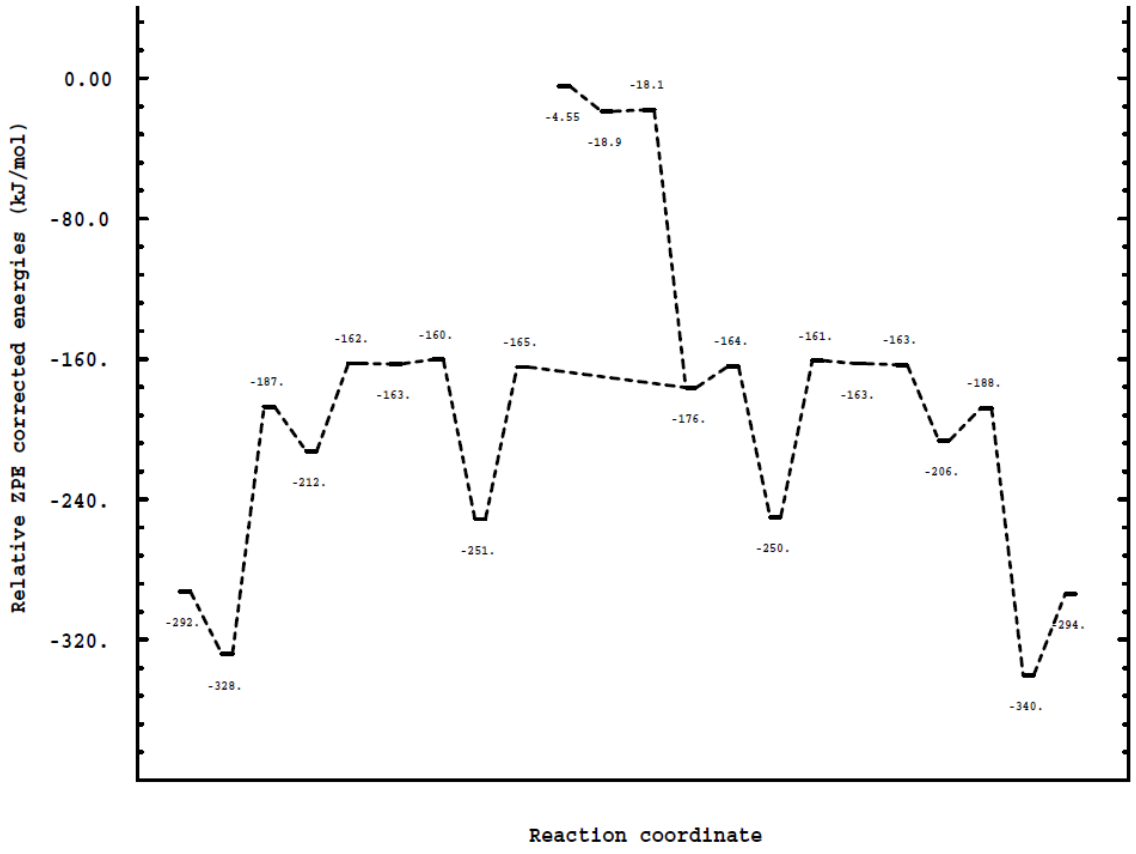

Figure 3.35: Energy diagram for MVK showing the possibility for branching

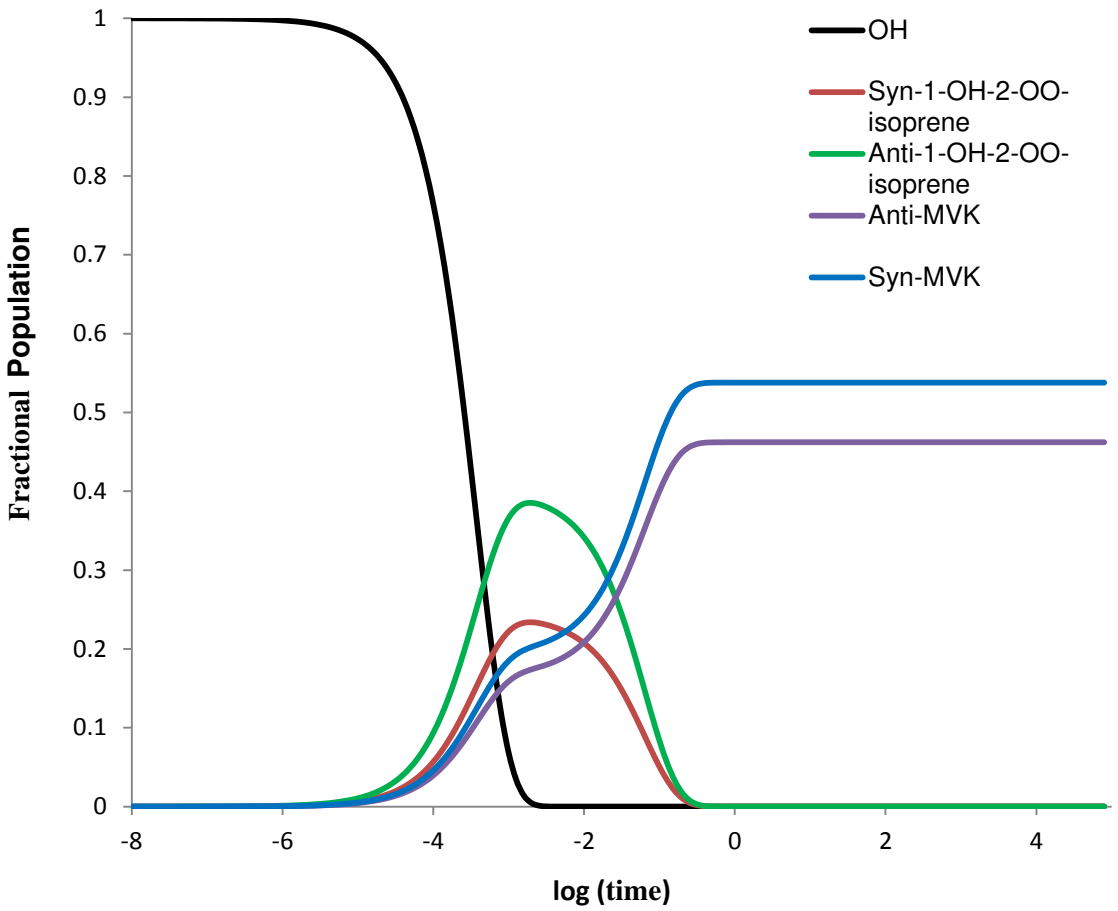

Figure 3.36: Product yields over time for MVK

Figure 3.34 gives a picture of the relative amounts of each species over time. At the beginning there is a high concentration of the hydroxyl radical. The concentration of the hydroxyl radical decreases rapidly once the intermediates and products begin to form. The 1-hydroxy-2-peroxy adducts are the only intermediate species to survive for any appreciable amount of time, all other species not listed are consumed as they are formed. Once the reaction has run to completion, or at infinite time, the final yields are 54% anti-MVK and 46% syn-MVK.

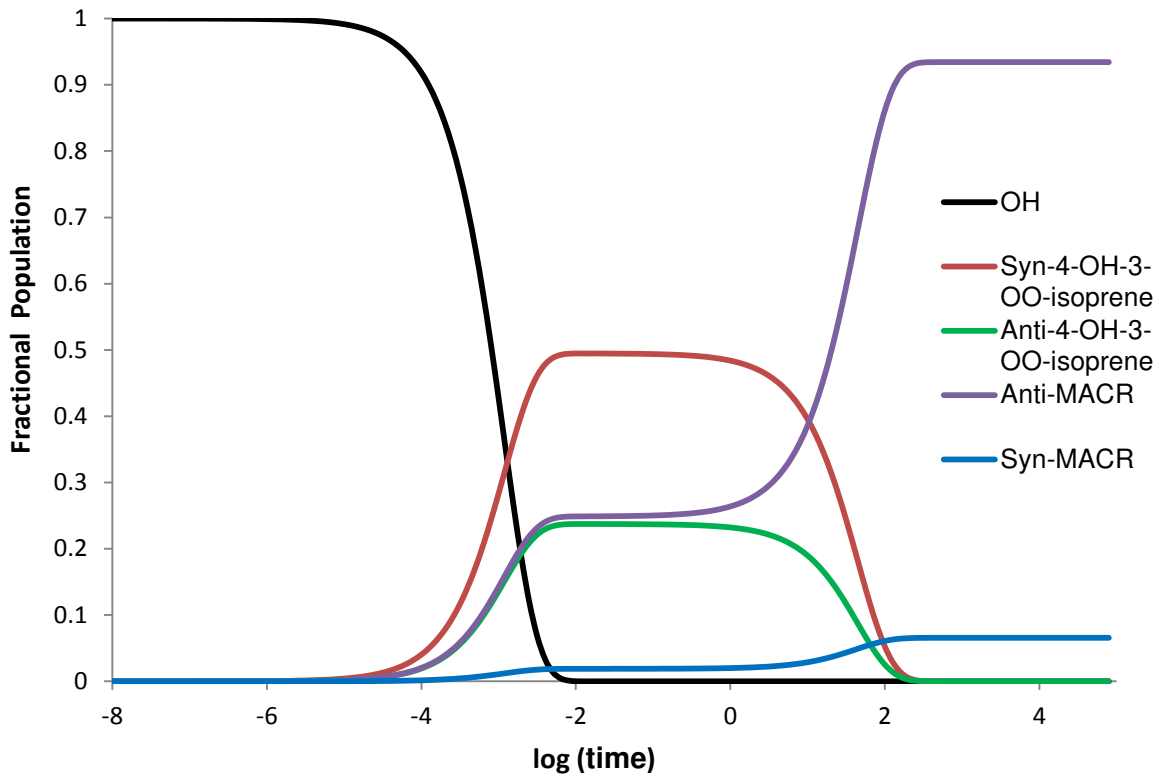

Figure 3.37: Product yields over time for MACR

As with MVK the hydroxyl radical is quickly consumed once intermediates and products begin to form. The intermediates for MACR are much longer lived compared to the life span of the MVK intermediates. The final yields are 93% for anti-MACR and 7% for syn-MACR. The 5 kcal/mol difference in the energies for TS4 is the reason for the very high preference for the anti-product as opposed to syn.

Product Molecules	**k (cm^3 $molecule^{-1}$ s^{-1})**
anti-mvk and syn-mvk	$2.7x10^{-11}$
anti-macr and syn-macr	$8.5x10^{-12}$

Table 2: Bimolecular rate constants for MACR and MVK reactions

Table 2 lists the overall rate constants for both the MVK and MACR reactions. The rate constant for MVK is about 3 times greater than the rate constant for MACR. This would indicate that MVK will be produced in greater amounts, however, to quantify how much more would be produced will require additional work. These values appear to be reasonable, and are comparable to values found in literature.(Park, Jongsma, Zhang, & North, 2004; 2004)

Conclusions

Four different reaction pathways were mapped out using the M062X density functional and both the 6-311++G** and maug-cc-PVTZ basis sets using a variety of techniques including NEB, DIMER, and MESMER. For syn- and anti-MVK the overall rate constant was found to be $2.7x10^{-11}$ cm^3 $molecule^{-1}$ s^{-1} and $8.5x10^{-12}$ cm^3 $molecule^{-1}$ s^{-1} for syn- and anti-MACR. The overall percent yields for syn- and anti-MVK are 54% and 46% respectively. For syn- and anti- MACR the percent yields are 7% and 91% respectively. Several of these results were compared against existing values found in literature and were found to be in good agreement. This study shows that three of the four explored reaction pathways are viable possibilities for the regeneration of the

hydroxyl radical during a hydroxyl facilitated isoprene oxidation. Due to the importance of isoprene and the hydroxyl radical, further studies on reactions involving both species is recommended. The next logical reaction pathway to study would be the 1,6-H shift pathway also proposed by Peeters.(Peeters et al., 2009)

References

Accelrys Software Inc. (2008). *Materials studio* (4.4th ed.). San Diego: Accelrys Software Inc.

Atkins, P. W., & De Paula, J. (2006). *Physical chemistry* (8th ed.). New York: Oxford university press.

Cramer, C. J. (2005). *Essentials of computational chemistry: Theories and models* (2nd ed.) Wiley. com.

Dunning, T. H., Jr. (1989). Gaussian basis sets for use in correlated molecular calculations. I. the atoms boron through neon and hydrogen. *Journal of Chemical Physics, 90*(2), 1007-23.

Eerdekens, G., Ganzeveld, L., Vilà-Guerau de Arellano, J., Klüpfel, T., Sinha, V., Yassaa, N., et al. (2009). Flux estimates of isoprene, methanol and acetone from airborne PTR-MS measurements over the tropical rainforest during the GABRIEL 2005 campaign. *Atmospheric Chemistry and Physics, 9*(13), 4207-4227. doi:10.5194/acp-9-4207-2009

Frisch, M. J., Trucks, G. W., Schlegel, H. B., Scuseria, G. E., Robb, M. A., Cheeseman, J. R., et al. *Gaussian 09 revision B.01*

Glowacki, D. R., Liang, C., Morley, C., Pilling, M. J., & Robertson, S. H. (2012; 2012). MESMER: An open-source master equation solver for multi-energy well reactions. *The Journal of Physical Chemistry A, 116*(38), 9545-9560.

Heyden, A., Bell, A. T., & Keil, F. J. (2005). Efficient methods for finding transition states in chemical reactions: Comparison of improved dimer method and partitioned rational function optimization method. *Journal of Chemical Physics, 123*(22), 224101/1-224101/14.

Jensen, F. (2006). *Introduction to computational chemistry* Wiley.

Jónsson, H., Mills, G., & Jacobsen, K. (1998). Nudged elastic band method for finding minimum energy paths of transition. *Classical and quantum dynamics in condensed phase simulations* (pp. 385-404) World Scientific.

Kohn, W., & Sham, L. J. (1965). Self-consistent equations including exchange and correlation effects. *Physical Review, 140*(4A), A1133-A1138.

Papajak, E., & Truhlar, D. G. (2010). Efficient diffuse basis sets for density functional theory. *Journal of Chemical Theory and Computation, 6*(3), 597-601.

Park, J., Jongsma, C. G., Zhang, R., & North, S. W. (2004; 2004). OH/OD initiated oxidation of isoprene in the presence of O2 and NO. *The Journal of Physical Chemistry A, 108*(48), 10688-10697.

Peeters, J., Nguyen, T. L., & Vereecken, L. (2009). HOx radical regeneration in the oxidation of isoprene. *Physical Chemistry Chemical Physics, 11*(28), 5935-5939.

Sheppard, D., Terrell, R., & Henkelman, G. (2008). Optimization methods for finding minimum energy paths. *The Journal of Chemical Physics, 128*(13)

Silva, G. d., Graham, C., & Wang, Z. (2009; 2009). Unimolecular beta-hydroxyperoxy radical decomposition with OH recycling in the photochemical oxidation of isoprene. *Environmental Science & Technology, 44*(1), 250-256.

Vereecken, L., & Francisco, J. S. (2012). Theoretical studies of atmospheric reaction mechanisms in the troposphere. *Chemical Society Reviews, 41*(19), 6259-6293.

Zhao, Y., & Truhlar, D. G. (2008). The M06 suite of density functionals for main group thermochemistry, thermochemical kinetics, noncovalent interactions, excited states, and transition elements: Two new functionals and systematic testing of four M06-class functionals and 12 other functionals. *Theoretical Chemistry Accounts, 120*(1-3), 215-241.